Modeling of Quantum Generators and Amplifiers on Semiconductor Materials

Biljana Veselinović[1], Milesa Srećković[2], Ivana Veselinović[3] and Milan Vlajnić[4]

***Abstract* –Analysis of characteristics for quantum well laser diode are presented in this paper. The performed analysis had been based on analytical and numerical calculations. Some adequate program from literature are modified and executed for given calculator architecture. The variation of principal lasing parameters is performed.**

***Keywords* – Quantum well lasers, p-n diode, Transparency threshold, Two-dimensional critical densities, Diode laser.**

I. INTRODUCTION

Lasers and amplifiers on semiconductor materials more and more replace other type of lasers. We can see almost daily apperance of come new semiconductor lasers with different coloring (blue, yellow, ...). The output of the other laser types were obtained, either directly, with parameter changes, or by Raman's or some other processes (frequency coupling), but output from small active material (comparing with large ionic and other lasers) were far better. On the one hand, this is in context of the semiconductor technologies papers, and on the other hand, semiconductor lasers work on many possible pumping ways. They can also be used as pumps with the other laser types.

After the first laser diodes, double heterostructure lasers, a line of quantum weel, quantum dot, quantum wire lasers appeared. There are also new types of VCSEL, VECSEL with a vertical resonators, etc. The main problems in all types are relations between laser characteristics: amplification, threshold, pump power, resonator configuration and efficiency. Efficiency is generally connected with pumping way, but here analysed type is type of active material that you should go theoretically and to aproach high levels of efficiency. Beside the general approaches, like with the other types that have these parameters, there are also some peculiarties with every separate type. Transparency threshold was chosen as a problem in this parer.

[1]Biljana Veselinović, Vinča Institute of Nuclear Sciences, Laboratory of computer sciences, P.O. Box 522, 11001, Belgrade, Serbia, Email:bilja@vin.bg.ac.yu

[2]Milesa Srećković, Belgrade University, Dept. Electric Engineering, Bulevar Kralja Aleksandra 73, 11000, Belgrade, Serbia, Email: Milesa@Tesla.rcub.bg.ac.yu

[3]Ivana Veselinović, BIA, Belgrade, Serbia, Email: ivancica1301@yahoo.com

[4]MilanVlajnić,YUBC System A.D., Dimitrija Tucovića 6, 11000, Belgrade, Serbia, Email:holydud@teleport.co.yu

II. TRANSPARENCY THRESHOLD

Fig. 1 shows the p-n diode which containing a single quantum well [1].

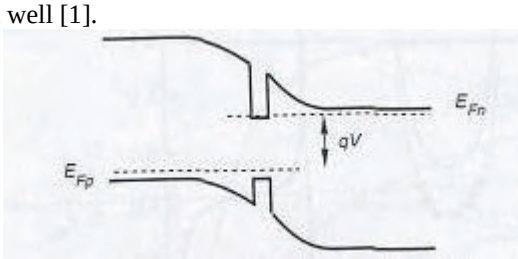

Fig. 1. A forward biased p-n diode containing a single quantum well.

Injected carriers accumulate in this well by forward biasing the diode. The carrier density per unit area n_s ,can be expressed as:

$$n_s = p_s = \frac{Jt_{tot}}{q}. \quad (1)$$

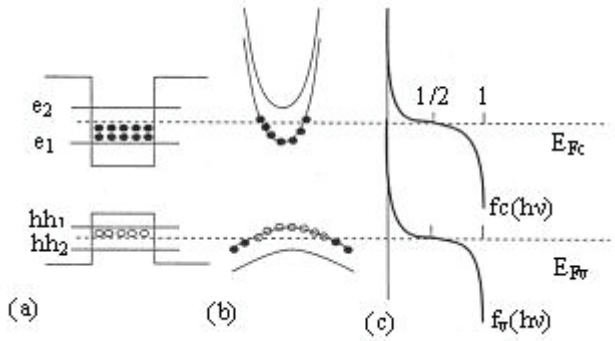

Fig. 2. Quantum well: a) band diagram; b) subband structure; c) associated Fermi-Dirac distributions;

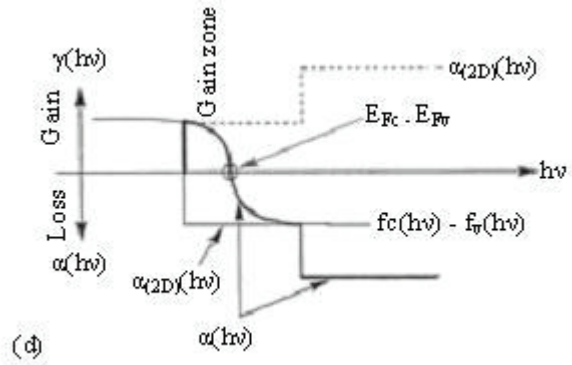

Fig. 2. Quantum well: d) gain curve

A population inversion which lead to transparency [4] in the quantum well (Fig. 2) can be obtained with a sufficiently elevated current densities. The quasi-Fermi levels begin to penetrate the subbands close to transparency. Only the n=m=1 subbands are involved. The gain can be expressed as:

$$\gamma(h\upsilon) = \alpha_{2D}\left[f_c^1(h\upsilon) - f_\upsilon^1(h\upsilon)\right]\theta(h\upsilon - E_g - e_1 - hh_1) \quad . \qquad (2)$$

The absorbtion coefficient α_{2D} (cm^{-1}) represent the absorbtion for a quantum well with zero population [1].

The quasi-Fermi levels, E_{Fc} i $E_{F\upsilon}$ are given by the conditions:

$$n_s = \int_{-\infty}^{\infty} \rho_{2D,e}(E)\, f_c^1(E)dE \,, \qquad (3)$$

$$n_s = \int_{-\infty}^{\infty} \rho_{2D,hh}(E)\left[1 - f_\upsilon^1(E)\right]dE \,. \qquad (4)$$

These conditions can be calculated precisely if the state densities for electrons ($\rho_{2D,e}$) and holes ($\rho_{2D,hh}$) are known. For electrons, Eqs. (3) and (4) can be expressed as:

$$n_s = \rho_{2D,e} \int_{E_g+e_1}^{+\infty} \frac{1}{1+\exp\left[(E - E_{FC})/kT\right]} dE \,, \qquad (5)$$

where the energy at the top of the valence band is taken to be zero. Setting $\exp((E - E_{Fc})/kT) = u$ and $\exp((E_g + e_1 - E_{Fc})/kT) = u_c$ Eq. (5) takes the form:

$$n_s = \rho_{2D,e} kT \int_{u_c}^{+\infty} \frac{1}{u(1+u)} du = \rho_{2D,e} kT \ln(1 + \frac{1}{u_c}) \,, \qquad (6)$$

so that:

$$n_s = n_c \ln\left[1 + \exp\left(\frac{E_{Fc} - E_g - e_1}{kT}\right)\right], \qquad (7)$$

$$n_s = n_\upsilon \ln\left[1 + \exp\left(\frac{hh_1 - E_{F\upsilon}}{kT}\right)\right], \qquad (8)$$

where , n_c and n_υ , are two-dimensional critical densities given by:

$$n_c = \rho_{2D,e} kT = \frac{m_e kT}{\pi\hbar^2} \,, \qquad (9)$$

$$n_\upsilon = \rho_{2D,hh} kT = \frac{m_{hh} kT}{\pi\hbar^2} \,. \qquad (10)$$

It will be shown that transparency and threshold densities can be expressed as a product of these two-dimensional critical densities by a factor close to 1, typical between 1 and 5.

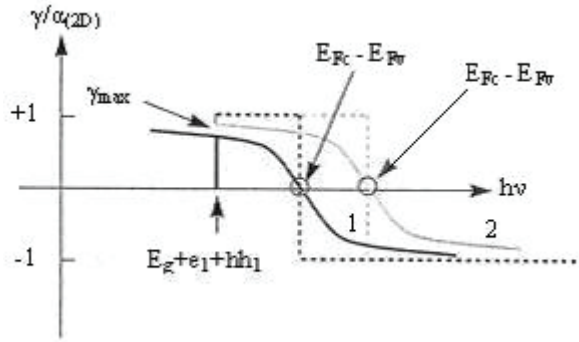

Fig. 3. Evolution of the gain curve for a quantum well laser for increasing pump currents.

The Fermi distributions in subbands n and m are given with:

$$f_c^n(h\nu) = \frac{1}{1+\exp\{[E_c^n(h\nu) - E_{Fc}]/kT\}} \,, \qquad (11)$$

$$E_c^n(h\nu) = E_g + e_n + \frac{m_r}{m_c}(h\nu - E_g - e_n) \,, \qquad (12)$$

$$f_c^m(h\nu) = \frac{1}{1+\exp\{[E_\nu^m(h\nu) - E_{Fc}]/kT\}} \,, \qquad (13)$$

$$E_c^m(h\nu) = -\frac{m_r}{m_\nu}(h\nu - E_g - hh_m) \,. \qquad (14)$$

We can calculate gain in this way: for a given current density J, calculate the carrier density (Eq. (1)), then quasi-Femi levels (Eqs. (7) and (8)),and finaly the gain with the help of (2) and Fermi functions (11-14). The gain curve as a function of photon energy for increasing carrier densities. is presented in Fig. 3. The dotted curves show the gain values at zero temperature. The black curves (1) correspond to low pump current conditions. The grey curves (2) correspond to high pump current conditions We note an abrupt increase in the gain for $h\upsilon > E_g + e_1 + hh_1$. The maximum gain $\gamma_{\max}$ is obtained when $h\upsilon = E_g + e_1 + hh_1$:

$$\gamma_{\max} = \alpha_{2D}\left[f_c^1(h\upsilon = E_g + e_1 + hh_1) -\right.$$

$$- f_{\upsilon}^{1}(h\upsilon = E_g + e_1 + hh_1)\Big]. \qquad (15)$$

Eqs. (7), (8) and (11-14) allow to relate the value of the Fermi function to the carrier density n_s:

$$1 - e^{-n_s/n_c} = 1 - \frac{1}{1+\exp\left[\left(E_{Fc} - E_g - e_1\right)/kT\right]} = f_c^1(E_g + e_1). \qquad (16)$$

Similarly:

$$e^{-p_s/n_c} = f_{\upsilon}^{1}(hh_1). \qquad (17)$$

The maximum gain can be writen as:

$$\gamma_{\max} = \alpha_{2D}(1 - e^{-n_s/n_c} - e^{-n_s/R_{c\upsilon}n_c}), \qquad (18)$$

where $R_{c\upsilon} = (m_{hh}/m_c)$ is the ratio of the effective masses for carriers in the conduction and valence bands.

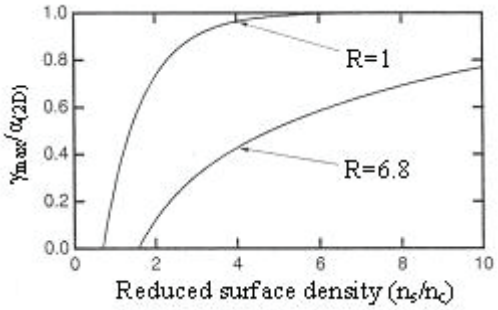

Fig. 4. Normalized gain as a function of normalized carrier surface density.

Fig. 4 shows the variation in maximum gain as a function of reduced carried surface density n_s/n_c with R=6.8 (GaAs) and R=1. It is obvious that the gain increases rapidly once the transparency condition has been reached, but saturates quickly. This results from the form of the two -dimensional density of states. From (14) the maximum gain becomes positive when the transparency threshold is reached once. When the transparency threshold n_{tr} is reached:

$$e^{-n_{tr}/n_c} + e^{-n_{tr}/R_{c\upsilon}n_c} = 1. \qquad (19)$$

For $R_{c\upsilon} = 1$, we have $n_{tr} = n_c \ln(2)$. The transparency current is always related to n_c by a numerical factor close to 1. It explains the importance of the concept of the two-dimensional density of states n_c. The transparency condition for different values of $R_{c\upsilon}$ is presented in Fig. 4. We note that it is advantageous to have closely matched effective masses between the valence and conduction bands.

The variation in maximum gain $\gamma_{\max}$, as a function of carrier surface density is logarithmic:

$$\gamma_{\max} = \gamma_0 \ln\left(\frac{n}{n_{tr}}\right), \qquad (20)$$

where the constant γ_0 depends only on the effective mass ratio $R_{c\upsilon}$. For values of n which approach the transparency threshold, the Eq. (20) leads to behaviours close to those predicted by (18).

III. Results of program P1

In order to analyze ratio between Eqs. (18) and (20) a procedure has been modeled and modified in MATHEMATICA program, given in the reference [1]. Equality presentation has been done using P1.

P1: Equality presentation between (18) and (20).

```
f = 1 - Exp[-x] - Exp[-x / R];
R = 6.8;
plot1 = Plot[f, {x, .5, 5}];
plot1 = Plot[f, {x, .5, 5},
   Frame → True, FrameLabel → {n / nc, γ / α2D},
   RotateLabel → False];
FindRoot[f == 0, {x, 1}];
x0 = x /. %;
g = Log[x / x0];
plot2 = Plot[0.48 * g, {x, .5, 5},
   Frame → True, FrameLabel → {n / nc, γ / α2D},
   RotateLabel → False];
Show[plot1, plot2]
```

The graphics shown in Fig. 5 are the results of execution of the program P1.

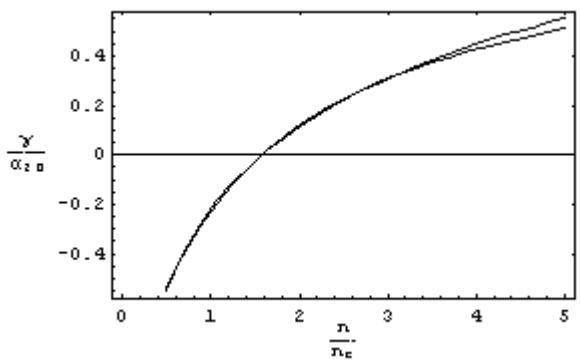

Fig. 5. Result of program P1

IV. ANALYSIS OF RESULTS

Fig. 5 compares expressions (18) and (20). By fitting, we find that $\gamma_0 = 0.48\alpha_{2D}$.

For GaAs, the two-dimensional state densities are:

$$\rho_{2D,e} = m_c / \pi\hbar^2 = 2.8x10^{13} cm^{-2} eV^{-1},$$

$$\rho_{2D,hh} = m_{hh} / \pi\hbar^2 = 1.9x10^{14} cm^{-2} eV^{-1}.$$

The two-dimensional critical density in the conduction band is $n_c = \rho_{2D,e} kT$ or $2.8x10^{13} cm^{-2} eV^{-1} x0.0259eV = 7.25x10^{11} cm^{-2}$. That is presented in Fig. 4. In GaAs, $n_{tr} = 1.6n_c = 1.16x10^{12} cm^{-2}$. In a 100Å (10 nm) wide quantum well, this coresponds to a transparency threshold density of $1.16x10^{18} cm^{-3}$. The result is very close to that obtained for bulk material. The advantage of using quantum wells structures does not involve decreasing the threshold carrier densities, but rather in decreasing the transparency current densities and hence the threshold current densities.

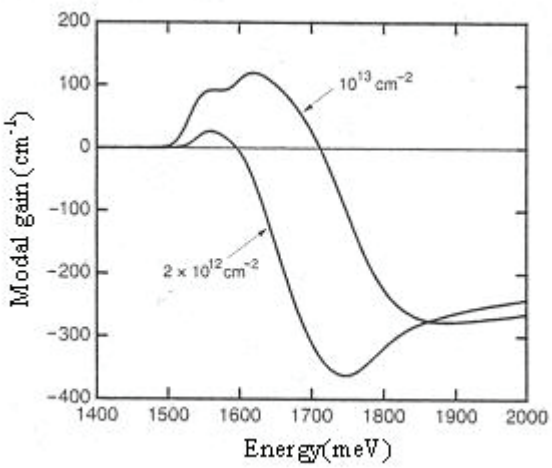

Fig. 6. Modal gain for a quantum well laser at two different carrier densities

The gain curve for a quantum-well laser is very complex. As the carrier densities increase in the wells, the electrons and holes populate higher energy states in the subbands and bring into play complex transitions: first the $e_1 - hh_1$ transitions, then $e_2 - hh_2$. Modal gain for a quantum well laser at two different carrier densities is presented in Fig. 6 shows. Both the $e_1 - hh_1$ and $e_2 - hh_2$ transitions can be observed under the higher current injection conditions .

IV. CONCLUSION

We analyzed the appropriate theories [1-7] and lasing condition. For the chosen model, we analyzed existing programming. For selected lasing parameters, we calculated maximum gain. The results correspond to the literature and the program works in defined domains.

REFERENCES

[1] E. Rosencher, B. Vinter,"Optoelectronics", Cambridge University Press, Cambrigge, 2002.
[2] http://www.iop.org/EJ/article/0268-1242/19/2/024/sst4_2_024.html
[3] N. Andrejev, Advanced Electronic Technologies and Systems Based on Low-Dimensional Quantum Devices, Elecronic edition.
[4] E. Kapon, Semiconductor Lasers I, Elecronic edition.
[5] I. Veselinović, M. Srećković, B. Veselinović, A. Đurđević, B. Stojković, “Non-linear Frequency Conversion Efficiency Analysis”, YU INFO 2007. Kopaonik.
[6] B. Veselinović, M. Srećković, I. Veselinović, M. Vlajnić, “Modeling of Semiconductor Laser Characteristics”, YU INFO 2007. Kopaonik.
[7] A. Yariv, *Quantum Electronics,*Willey, New York, 1989.